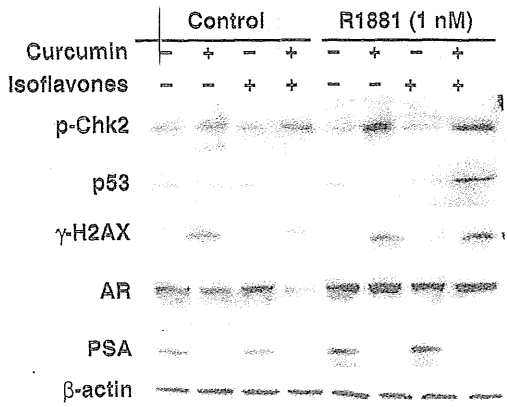

Fig. 3. Testosterone induced the activation of the DNA damage response under the treatment of 25 μM curcumin. AR, androgen receptor; p-Chk2, phosphorylated-Chk2; PSA, prostate-specific antigen.

analysis, LNCaP cells were cultured in a serum-free medium for 2 days prior to the addition of androgens. Figure 3 shows that the phosphorylation of CHK, H2AX and p53 was induced by 1 nM R1881 in LNCaP cells treated with 25 μM curcumin, which express the androgen receptor. Isoflavones did not induce testosterone-mediated activation of the DDR. The expression of androgen receptor and PSA was increased by 1 nM R1881 as reported previously.[19,20] Curcumin suppressed the expression of PSA even in cells treated with 1 nM R1881 (Fig. 3).

PARP cleavage was induced by testosterone with curcumin. To verify the mechanism by which testosterone enhanced the DDR with curcumin, the expression of apoptosis-related proteins was monitored by western blot analysis (Fig. 4). Occurrence of PARP cleavage, a marker of apoptosis,[21] occurred in curcumin-treated cells. We could not observe the induction of Chk2 and PARP cleavage by 1 μM DHT when the cells were treated with 25 μM curcumin. However, PARP cleavage was induced by 1 μM DHT in combination with a higher concentration, 50 μM curcumin. Densitometric analysis showed that 50 μM curcumin with 1 μM DHT induced the phosphorylation of Chk2 (4.4-fold) and PARP cleavage (2.4-fold), respectively, when compared with 50 μM curcumin without 1 μM DHT. This testosterone-induced PARP cleavage was decreased by the addition of 10 μM flutamide, which is an inhibitor of the androgen receptor. Densitometric analysis showed that the treatment of flutamide reduced the phosphorylation of Chk2 (8.2-fold) and PARP cleavage (16.9-fold), respectively, when compared with 50 μM curcumin with 1 μM DHT. These results suggest that DHT enhance apoptosis through the DDR when combined with a higher concentration of curcumin, which is dependent on signaling mediated by the androgen receptor.

Discussion

Curcumin is extensively used as a spice or pigment in the Asian diet, especially in curry. An epidemiological study showed that a low incidence of large bowel cancer in Indians can be attributed to the intake of curcumin.[22] Animal studies revealed that dietary administration of curcumin inhibited the incidence of cancers.[23] Curcumin is under clinical trials mainly for various cancers and related diseases.[23] In *in vivo* analyses, curcumin has been shown to cause apoptosis and cell cycle arrest with inhibited cell growth, activation of signal transduction, and transforming activities in both androgen-dependent and independent prostate cancer cells.[5,6] Curcumin has anti-inflammatory and antioxidant properties through inhibiting the activation of NF-κB, reducing COX-2 and AKT, decreasing the production of IL-6.[24–27] Recent evidence suggests that genistein induces the DDR through ATM.[28] There is a report that curcumin induces the phosphorylation of ATM in pancreatic cancer cells.[29] To our knowledge, this is the first report that isoflavones and curcumin activate the DDR, such as the phosphorylation of ATM, histone H2AX, Chk2 and p53 proteins, in LNCaP cells. DNA damage checkpoints are activated in the early stages of human tumorigenesis, leading to cell-cycle blockade or apoptosis and thereby inhibiting tumour progression.[8] Thus, polyphenols such as isoflavones and curcumin might contribute to the prevention of prostate cancer by activating a DDR. The reduced incidence of prostate cancers in several Asian populations may be due to the additive effects of several compounds including curcumin and isoflavones commonly found in Asian foods.

Another finding of the present study was that testosterone enhanced apoptosis of LNCaP cells through a curcumin-induced DDR that was dependent on the androgen receptor. Several lines of study have shown that testosterone has a dual role of promoting both proliferation and differentiation in androgen-dependent prostate cancer cells.[30,31] A previous study has shown that testosterone mediates cellular proliferation signals in the prostate through increased expression of Skp2, the ubiquitin ligase that targets p27 for degradation,[32] while testosterone induces the cyclin-dependent kinase inhibitor p21Cip1.[33]

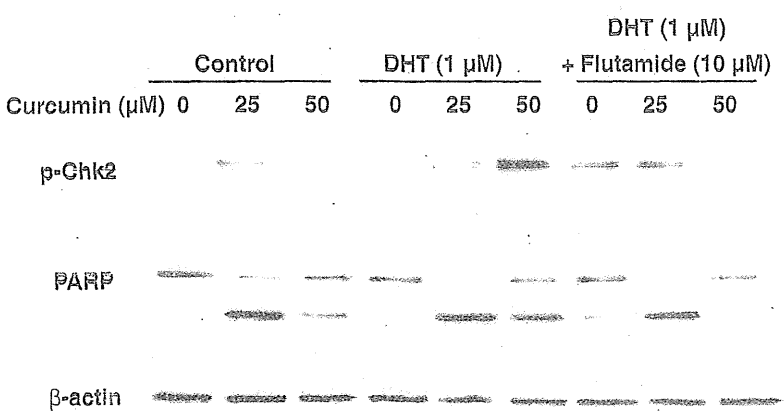

Fig. 4. Testosterone induced poly (ADP-ribose) polymerase (PARP) cleavage with activation of Chk2. Immunoblots were probed for mouse anti-human β-actin antibody as an internal control. DHT, dihydrotestosterone; p-Chk2, phosphorylated-Chk2.

doi: 10.1111/j.1349-7006.2010.01791.x

Our data demonstrated that in combination with curcumin testosterone lost its proliferative effect on LNCaP cells and contributed to a DDR. Currently, androgen deprivation is the gold standard for the treatment of metastatic prostate cancer. However, this treatment has the limitation that many of these cancers eventually become androgen independent, and the deprivation of androgen may cause serious morbidities, including obesity, hypertension and osteoporosis.[34] Therefore, our findings might have clinical implications for the development of new strategies for the prevention and treatment of prostate cancer that do not depend on androgen deprivation. The mechanism underlying this curcumin-induced testosterone-enhanced DDR warrants further study.

The present study also showed that certain combinations of polyphenols worked additively. It is both reasonable and practical to combine such components in daily diets rather than take single constituents daily to prevent the onset of cancer.

In conclusion, a combined treatment of soy isoflavones and curcumin additively induced a DDR in cultured prostate cancer cells. In addition, testosterone enhanced signals of DDR markers induced by curcumin treatment. Our findings suggest a potential protective effect of curcumin treatment against prostate carcinogenesis.

References

1 Hebert JR, Hurley TG, Olendzki BC, Teas J, Ma Y, Hampl JS. Nutritional and socioeconomic factors in relation to prostate cancer mortality: a cross-national study. *J Natl Cancer Inst* 1998; **90**: 1637–47.
2 Guo W, Kong E, Meydani M. Dietary polyphenols, inflammation, and cancer. *Nutr Cancer* 2009; **61**: 807–10.
3 Ohga N, Hida K, Hida Y *et al.* Inhibitory effects of epigallocatechin-3 gallate, a polyphenol in green tea, on tumor-associated endothelial cells and endothelial progenitor cells. *Cancer Sci* 2009; **100**: 1963–70.
4 Bektic J, Guggenberger R, Eder IE *et al.* Molecular effects of the isoflavonoid genistein in prostate cancer. *Clin Prostate Cancer* 2005; **4**: 124–9.
5 Teiten MH, Gaascht F, Eifes S, Dicato M, Diederich M. Chemopreventive potential of curcumin in prostate cancer. *Genes Nutr* 2010; **5**: 61–74.
6 Dorai T, Gehani N, Katz A. Therapeutic potential of curcumin in human prostate cancer-I. curcumin induces apoptosis in both androgen-dependent and androgen-independent prostate cancer cells. *Prostate Cancer Prostatic Dis* 2000; **3**: 84–93.
7 Ide H, Tokiwa S, Sakamaki K *et al.* Combined inhibitory effects of soy isoflavones and curcumin on the production of prostate-specific antigen. *Prostate* 2010; **70**: 1127–33.
8 Bartkova J, Horejsi Z, Koed K *et al.* DNA damage response as a candidate anti-cancer barrier in early human tumorigenesis. *Nature* 2005; **434**: 864–70.
9 Gorgoulis VG, Vassiliou LV, Karakaidos P *et al.* Activation of the DNA damage checkpoint and genomic instability in human precancerous lesions. *Nature* 2005; **434**: 907–13.
10 Bartek J, Bartkova J, Lukas J. DNA damage signalling guards against activated oncogenes and tumour progression. *Oncogene* 2007; **26**: 7773–9.
11 Sugimura Y, Cunha GR, Donjacour AA. Morphogenesis of ductal networks in the mouse prostate. *Biol Reprod* 1986; **34**: 961–71.
12 Cunha GR, Ricke W, Thomson A *et al.* Hormonal, cellular, and molecular regulation of normal and neoplastic prostatic development. *J Steroid Biochem Mol Biol* 2004; **92**: 221–36.
13 Morgentaler A. Testosterone and prostate cancer: an historical perspective on a modern myth. *Eur Urol* 2006; **50**: 935–9.
14 Yamamoto S, Yonese J, Kawakami S *et al.* Preoperative serum testosterone level as an independent predictor of treatment failure following radical prostatectomy. *Eur Urol* 2007; **52**: 696–701.
15 Morgentaler A, Bruning CO 3rd, DeWolf WC. Occult prostate cancer in men with low serum testosterone levels. *JAMA* 1996; **276**: 1904–6.
16 Isom-Batz G, Bianco FJ Jr, Kattan MW, Mulhall JP, Lilja H, Eastham JA. Testosterone as a predictor of pathological stage in clinically localized prostate cancer. *J Urol* 2005; **173**: 1935–7.
17 Massengill JC, Sun L, Moul JW *et al.* Pretreatment total testosterone level predicts pathological stage in patients with localized prostate cancer treated with radical prostatectomy. *J Urol* 2003; **169**: 1670–5.
18 Nishiyama T, Ikarashi T, Hashimoto Y, Suzuki K, Takahashi K. Association between the dihydrotestosterone level in the prostate and prostate cancer aggressiveness using the Gleason score. *J Urol* 2006; **176**: 1387–91.
19 Kemppainen JA, Lane MV, Sar M, Wilson EM. Androgen receptor phosphorylation, turnover, nuclear transport, and transcriptional activation. Specificity for steroids and antihormones. *J Biol Chem* 1992; **267**: 968–74.
20 Schuur ER, Henderson GA, Kmetec LA, Miller JD, Lamparski HG, Henderson DR. Prostate-specific antigen expression is regulated by an upstream enhancer. *J Biol Chem* 1996; **271**: 7043–51.
21 Soldani C, Scovassi AI. Poly(ADP-ribose) polymerase-1 cleavage during apoptosis: an update. *Apoptosis* 2002; **7**: 321–8.
22 Mohandas KM, Desai DC. Epidemiology of digestive tract cancers in India. V. Large and small bowel. *Indian J Gastroenterol* 1999; **18**: 118–21.
23 Duvoix A, Blasius R, Delhalle S *et al.* Chemopreventive and therapeutic effects of curcumin. *Cancer Lett* 2005; **223**: 181–90.
24 Mukhopadhyay A, Bueso-Ramos C, Chatterjee D, Pantazis P, Aggarwal BB. Curcumin downregulates cell survival mechanisms in human prostate cancer cell lines. *Oncogene* 2001; **20**: 7597–609.
25 Plummer SM, Holloway KA, Manson MM *et al.* Inhibition of cyclo-oxygenase 2 expression in colon cells by the chemopreventive agent curcumin involves inhibition of NF-kappaB activation via the NIK/IKK signalling complex. *Oncogene* 1999; **18**: 6013–20.
26 Tsui KH, Feng TH, Lin CM, Chang PL, Juang HH. Curcumin blocks the activation of androgen and interlukin-6 on prostate-specific antigen expression in human prostatic carcinoma cells. *J Androl* 2008; **29**: 661–8.
27 Lin L, Hutzen B, Ball S *et al.* New curcumin analogues exhibit enhanced growth-suppressive activity and inhibit AKT and signal transducer and activator of transcription 3 phosphorylation in breast and prostate cancer cells. *Cancer Sci* 2009; **100**: 1719–27.
28 Ye R, Goodarzi AA, Kurz EU *et al.* The isoflavonoids genistein and quercetin activate different stress signaling pathways as shown by analysis of site-specific phosphorylation of ATM, p53 and histone H2AX. *DNA Repair (Amst)* 2004; **3**: 235–44.
29 Sahu RP, Batra S, Srivastava SK. Activation of ATM/Chk1 by curcumin causes cell cycle arrest and apoptosis in human pancreatic cancer cells. *Br J Cancer* 2009; **100**: 1425–33.
30 Gao J, Arnold JT, Isaacs JT. Conversion from a paracrine to an autocrine mechanism of androgen-stimulated growth during malignant transformation of prostatic epithelial cells. *Cancer Res* 2001; **61**: 5038–44.
31 Isaacs JT, Isaacs WB. Androgen receptor outwits prostate cancer drugs. *Nat Med* 2004; **10**: 26–7.
32 Waltregny D, Leav I, Signoretti S *et al.* Androgen-driven prostate epithelial cell proliferation and differentiation in vivo involve the regulation of p27. *Mol Endocrinol* 2001; **15**: 765–82.
33 Lu S, Liu M, Epner DE, Tsai SY, Tsai MJ. Androgen regulation of the cyclin-dependent kinase inhibitor p21 gene through an androgen response element in the proximal promoter. *Mol Endocrinol* 1999; **13**: 376–84.
34 Sharifi N, Gulley JL, Dahut WL. Androgen deprivation therapy for prostate cancer. *JAMA* 2005; **294**: 238–44.

Hemodialysis International 2012; 16:320–321

Letters to the Editor

The impact of the Great Tohoku Earthquake on the dialysis practice in the disaster-stricken area

To the Editor:

The Great Tohoku Earthquake on March 11 and ensuing tsunami has caused devastation in Japan. While the earthquake was the biggest in the Japan's recorded history, little information is available regarding its impact on the dialysis practice in the developed countries. Herein, we report our experience to show the chaotic situations of dialysis practice in our country.

Patients who required the most emergent medical attention were those with end-stage renal disease (ESRD). This finding was comparable to other natural disasters such as hurricanes.[1] ESRD was common in an aging society such as in Japan. More than 10,000 of patients with ESRD could not receive dialysis in the disaster area due to shortage of medicine, disrupted water supply, and blackouts. Without dialysis, they would be fatal within several days. It was critical to ensure the availability of dialysis for these patients; however, hospitals in neighboring affected area were not capable of accepting these patients due to the exhaustion of medical resources. Thus, these situations gave rise to an urgent need of dialysis patients' transportation to hospitals in unaffected areas.

Of note, the local governments were severely damaged by the earthquake and tsunami, and the normal administration system could not work in the disaster area. In Japan, most physicians use social network services such as mailing lists, Twitter, and Facebook. These technologies played an important role in sharing information among physicians after the earthquake and tsunami.

Seventeen physicians in Tokiwakai group in Iwaki, Fukushima Prefecture, who cared patients with ESRD suffered from the disaster. While no dialysis patients were injured because of the earthquake itself, continuation of dialysis was difficult after earthquake and tsunami due to damage to the dialysis facilities, shortage of water and electricity supply. They sought some help for patient transfer, and contacted us. The countermeasures had not been taken to such a major catastrophe before the earthquake. Thus, we established "Earthquake Medical Network" on March 14, and tried to transfer 584 dialysis patients from Iwaki to Tokyo, Chiba, and Niigata. Baseline characteristics of dialysis patients were shown in Table 1. Twelve doctors were involved in the transportation.

Table 1 Baseline charcteristics of dialysis patients and information on transportation

Characteristics	(n = 584)
Age, median (range), y	67 (20–93)
>= 65	317
< 65	267
Sex	
Male	379
Female	205
Primary reason kidneys failed	
Diabetic nephropathy	205
Hypertensive nephrosclerosis	31
Glomerulonephritis	97
Polycystic kidney disease	14
Obstructive uropathy	2
Other	16
Unknown	219
Years since 1st ESRD (range), y	4.6 (0.0–71.4)
Transport Distance (range), km	181.4 (160.9–274.2)
Interval between dialyses which patients were forced to wait for due to evacuation (range), d	3 (1–10)

The difficulty lay in securing transportation measures, places where patients and their families stayed, and

Correspondence to: M. Tsubokura, MD, Division of Social Communication System for Advanced Clinical Research, Institute of Medical Science, University of Tokyo, 4-6-1 Shirokanedai, Minato-ku, Tokyo, Japan.
E-mail: tsubokura-tky@umin.ac.jp

Conflicts of interests: None declared.

DOI:10.1111/j.1542-4758.2011.00655.x

hospitals that would accept these patients. In particular, securing buses and gasoline were extremely difficult. While no authority funded the volunteer transfers, coordination was conducted through physicians' networks outside the disaster area. In responses to our requests, several bus lines, hotels, and hospitals containing dialysis units announced cooperation. Finally, the transportation was successfully completed without any deaths of patients on March 16 with 3 days median interval between dialyses, which patients were forced to wait. While the detailed information on the symptoms accompanied by the transportation was not available, no severe symptoms were reported other than hyperkalemia and volume overload. Two doctors were remained in the stricken area without any injury from the disaster.

With the median evacuation period of 17 days (range 1–184 days), 499 of 584 evacuees with ESRD were confirmed moving back to their hometown dialysis center as of October 2011.

Our experience suggests that continuation of dialysis is difficult after earthquake and tsunami. The only option in such scenarios is to transfer patients to undamaged areas in order to continue treatment. Since the conventional administration system does not work, cooperation of medical professionals through social networks is critical to accomplish it.

Masaharu TSUBOKURA, MD[1] Shigeo HORIE, MD[2]
Hideki KOMATSU, MD[3] Michio TOKIWA, MD[4]
Masahiro KAMI, MD[1]
[1]*Division of Social Communication System for Advanced Clinical Research, Institute of Medical Science, University of Tokyo, Tokyo, Japan;*
[2]*Department of Urology, Teikyo University School of Medicine, Tokyo, Japan;*
[3]*Department of Urology, Kameda Medical Center, Chiba, Japan;* [4]*Tokiwa-kai Group, Iwaki, Japan*

REFERENCE

1 Kenney RJ. Emergency preparedness concepts for dialysis facilities: Reawakened after Hurricane Katrina. *Clin J Am Soc Nephrol.* 2007; 2:809–813.

The Prostate 72:1407–1411 (2012)

Testosterone Promotes DNA Damage Response Under Oxidative Stress in Prostate Cancer Cell Lines

Hisamitsu Ide,* Yan Lu, Jingsong Yu, Toshiyuki China, Tomoka Kumamoto, Tatsuro Koseki, Raizo Yamaguchi, Satoru Muto, and Shigeo Horie

Department of Urology, Teikyo University School of Medicine, Itabashi-ku, Tokyo, Japan

BACKGROUND. Sustained chronic inflammation and oxidative stress in the prostate promote prostate carcinogenesis. The process of oncogenic transformation leads to enhanced DNA damage and activates the checkpoint network that functions as an inducible barrier against cancer progression. Here, we analyzed the effects of testosterone on the DNA damage response in prostate cancer cells to assess whether testosterone functions a barrier to cancer progression under the oxidative stress.

METHODS. We examined the effects of testosterone on components of the DNA damage response pathway, including ATM (ataxia-telangiectasia-mutated kinase), H2AX (histone H2AX variant), and Chk2 (checkpoint kinase2) in prostate cancer cell lines, treated with various concentration of hydrogen peroxide (H_2O_2). Cellular apoptosis was quantified by poly (ADP-ribose) polymerase (PARP) cleavage and flow cytometry.

RESULTS. H_2O_2 induced apoptosis and phosphorylation of ATM, Chk2, and H2AX in LNCaP cells. An ATM inhibitor, Ku55933, reduced H_2O_2-induced apoptosis in LNCaP and 22Rv1 cells. Androgen treatments increased H_2O_2-induced activation of the DNA damage response and PARP cleavage, but not when the H_2O_2-treated cells were also treated with the anti-androgen flutamide. The ATM inhibitor Ku55933 inhibited androgen-induced phosphorylation of ATM and PARP cleavage.

CONCLUSIONS. DNA damage responses play important roles in the maintenance of the cell homeostasis in response to oxidative stress. Our results indicated that under oxidative stress androgen signaling may induce apoptosis by activating the DNA damage response.

Prostate 72:1407–1411, 2012. © 2012 Wiley Periodicals, Inc.

KEY WORDS: prostate cancer; oxidative stress; testosterone; androgen receptor; DNA damage response

INTRODUCTION

In prostate cancer, testosterone obviously stimulates the proliferation of cells. However, prostate cancer is more common in older men, who have declining testosterone levels. Large pooled analysis did not show an association between high circulating levels of testosterone and prostate cancer risk [1]. Moreover, several lines of evidence suggest that decreases in testosterone level accelerate the progression of prostate cancer. Low testosterone levels are associated with an advanced tumor stage at presentation, positive surgical margins, high Gleason scores, and worse overall survival [2]. Furthermore, several clinical studies showed that prostate cancer patients responded to exogeneous testosterone therapy [3,4]. These observations indicate that testosterone may have protective effects against prostate carcinogenesis and malignant transformation.

The associations of aging with prostate cancer and aging with oxidative stress are well described. Reactive oxygen stress (ROS) has been implicated in prostate carcinogenesis, and repair of oxidative DNA damage may be defective in prostate tissues as a result of uncontrolled oxidative stress and increased

*Correspondence to: Hisamitsu Ide, MD, PhD, Department of Urology, Teikyo University School of Medicine, 2-11-1 Kaga, 2-chome, Itabashi-ku, Tokyo 173-8605, Japan.
E-mail: ihisamit@med.teikyo-u.ac.jp
Received 6 May 2011; Accepted 20 December 2011
DOI 10.1002/pros.22492
Published online 30 January 2012 in Wiley Online Library (wileyonlinelibrary.com).

oxidative DNA damage [5,6]. Recently, DNA damage response pathways were shown to have a major role in tumor progression and suppression of prostate cancer [7]. Agents that cause DNA double-strand breaks (DSB), including ROS, induce ataxia-telangiectasia-mutated kinase (ATM)-mediated phosphorylation and the resulting activation of Chk2 (checkpoint kinase2). Activated ATM sets off a cascade of downstream events, including phosphorylation of histone H2AX (γH2AX) and phosphorylation/stabilization of p53, that lead to cell cycle arrest and repair of DNA damage or to apoptosis if the DNA damage is too severe to be repaired [8]. Importantly, recent studies demonstrate that this pathway is constitutively activated in a wide range of premalignant lesions and low-grade cancers. Indeed, ATM and Chk2 are specifically activated in prostatic intraepithelial neoplasias (PINs), which may be a precursor of prostate cancer [9]. Thus, activation of DNA damage response signaling may have an important role as an inducible barrier that inhibits the progression of prostate carcinogenesis. While oxidative stress is known to induce the DNA damage response, the effects of testosterone on DNA damage signaling are unknown. The present study was designed to investigate whether testosterone is capable of influencing the DNA damage response signaling pathway in LNCaP and 22Rv1, androgen sensitive human prostate cancer cell lines. Our results may indicate that testosterone may suppress prostate carcinogenesis through the activation of DNA damage response.

MATERIALS AND METHODS

Cell Culture and Reagents

LNCaP and 22Rv1, human prostate cancer cell lines, were obtained from the American Type Culture Collection (Rockville, MD). The cells were routinely maintained in RPMI 1640 supplemented with 10% FCS, 100 units/ml penicillin, and 100 μg/ml streptomycin. Cells were cultured at 37°C in a humidified incubator with 5% CO_2. Hydrogen peroxide (H_2O_2,Wako, Tokyo, Japan) was diluted in the culture medium at various concentrations. For the androgen stimulation analysis, the cells were cultured in a serum-free medium for 2 days prior to the addition of various concentration of dihydrotestosterone (Wako, Tokyo, Japan) or synthetic androgen R1881 (New England Nuclear, Boston, MA). To block androgen signaling, the cells were cultured with flutamide (Sigma-Aldrich Co., St. Louis, MO). To block ATM phosphorylation, the cells were cultured with an ATM inhibitor, ku55933 (Sigma-Aldrich Co., St. Louis, MO). To block Chk2 phosphorylation, the cells were cultured with Chk2 inhibitor 2 (Sigma-Aldrich Co., St. Louis, MO). The levels of oxidized DNA as indicated by 8-hydroxy-2′-deoxyguanosine (8-OHdG) were measured by enzyme-linked immunosorbent assay (ELISA) (8-OHdG check high sensitivity kit, Japan Institute for the Control of Aging, Fukuoka, Japan).

Immunohistochemsitry

Serial 4-μm-thick sections of prostate tissues were deparaffinized in three changes of xylene and rehydrated through a graded series (decreasing from 100 to 70%) of ethanol in water. The sections were immersed in citrate buffer (pH 6.0) and autoclaved at 120°C for 5 min and then placed in 3% H_2O_2 in methanol for 20 min at room temperature to block endogenous peroxidase activity. Nonspecific protein binding was blocked by incubating the section for 30 min to 1 h in 5% goat serum. Next, the sections were incubated overnight at 4°C in mouse anti-human 8-OHdG antibody (JaICA, Nikken SEIL Co., Ltd., Shizuoka, Japan). Sections were then processed for immunohistochemistry using the EnVisionTM+ system (DAKO, Glostrup, Denmark).

Immunoblotting

Subconfluent cells were treated with various concentrations of H_2O_2. Cells were washed twice with cold PBS and then lysed in RIPA buffer supplemented with complete EDTA-free Protease Inhibitor Cocktail (Roche Applied Science, Mannheim, Germany) and PhosStop Phosphatase Inhibitor Cocktail (Roche Applied Science) on ice for 30 min. The cell lysates were sonicated five times for 10 sec each time and centrifuged at 11,000*g* for 30 min at 4°C, and the supernatants were collected. Protein concentrations were measured using a BCA protein assay kit (Pierce Inc., Rockford, IL). Protein samples were separated by SDS–PAGE and transferred to a PVDF membrane (Millipore Inc., Tokyo, Japan). Immunoblotting was performed using a rabbit anti-androgen receptor antibody (Santa Cruz Biotechnology Inc., CA; 1:2,000), rabbit anti-phospho-ATM (Ser1981) antibody (Rockland Immunochemicals Inc., Gilbertsville, PA; 1:2,000), rabbit anti-phospho-Chk2 (Thr68) antibody (Cell Signaling Technology Inc., Danvers, MA; 1:1,000), rabbit anti-phospho-p53 (Ser15) antibody (Cell Signaling Technology; 1:1,000), rabbit anti-phospho-H2AX (Ser139) antibody (Upstate Inc., Temecula, CA; 1:1,000 dilution), or rabbit anti-poly (ADP-ribose) polymerase (PARP) antibody (Cell Signal Technology; 1:1,000 dilution); a mouse anti-human β-actin antibody (Sigma-Aldrich Co., St. Louis, MO; 1:10,000 dilution) was used to measure β-actin, which functioned as an internal loading control. Immunoreactive proteins were visualized with ECL detection reagents

(GE Healthcare Biosciences, Tokyo, Japan). The results of western blotting were quantified by densitometric analysis using an LAS 3000 Densitometer and Multi Gauge v3.1 (Fujifilm, Tokyo, Japan). All protein values were normalized to β-actin values.

Determination of Apoptosis by Flow Cytometry

The FITC Annexin V Apoptosis Detection kit (BD Pharmingen, San Diego, CA) was used to determine the extent of apoptosis in LNCaP cultures. Cell suspensions were transferred to 5-ml polypropylene tubes, and 5 ml each of PI (50 mg/ml stock) and annexin V-FITC were added simultaneously to each tube. Annexin V-positive but PI-negative cells were defined as early apoptotic cells; annexin V-positive and PI-positive cells were defined as late apoptotic or necrotic cells. After incubation in the dark at room temperature for 15 min, the cells were analyzed by flow cytometry (FACSCalibur system, BD Biosciences, San Joe, CA).

RESULTS

Detection of 8-OHdG in Prostate Cancer

Of the several approaches to the measurement of oxidative DNA damage, the measurement of 8-OHdG, which results from oxidative stress, is very reliable and widely accepted [10]. The immunohistochemical study using 8-OHdG antibodies revealed positive staining in nuclei of prostate epithelial cells and prostate cancer cells (Fig. 1A). This result indicated that the prostate may be particularly vulnerable to oxidative attack. We measured 8-OHdG in LNCaP cells after 24-h treatment with various concentrations of H_2O_2 as a model of oxidative stress. Significant H_2O_2-dependent increases in 8-OHdG levels were observed in LNCaP cells (Fig. 1B).

Activation of DNA Damage Response and Apoptosis by Oxidative Stress

To evaluate the DNA damage response that was induced in prostate cancer cells by oxidative stress, we examined the phosphorylation of ATM, CHK2, and H2AX using immunoblotting with phosphor-specific antibodies. LNCaP cells were treated with various concentration of H_2O_2, and there was a dose-dependent response in the phosphorylation levels of these proteins to H_2O_2 treatment (Fig. 2). When we used 100 μM H_2O_2 to induce apoptosis, there were 34% more apoptotic cells in the H_2O_2-treated cells than in the untreated cell based on the flow cytometry analysis. The ATM inhibitor Ku55933 and a Chk2 inhibitor reduced the number of apoptotic

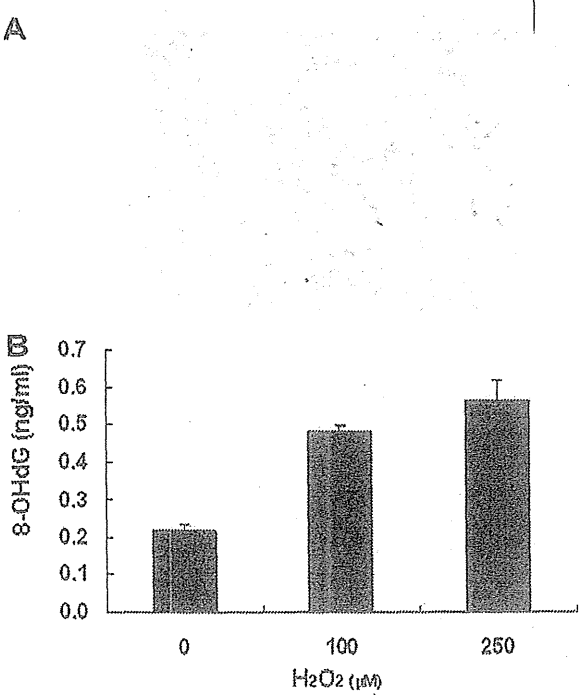

Fig. 1. Evaluation of oxidative stress in prostate cancer cells based on 8-OHdG levels. **A**: Detection of 8-OHdG in prostate cancer tissues by immunohistochemistry (**B**) Increasing 8-OHdG in LNCaP cells treated with various concentration of H_2O_2 detected by ELISA. [Color figure can be seen in the online version of this article, available at http://wileyonlinelibrary.com/journal/pros]

cells by a reduction from 38 to 29%, and 38 to 24%, respectively (data not shown). These results indicated that some of the apoptosis induced by H_2O_2 treatment was depended by the DNA damage response pathway.

Induction of DNA Damage Response and PARP Cleavage by Testosterone

Activation of the DNA damage response pathway and PARP cleavage was increased by 1 nM synthetic androgen R1881. Densitometric analysis showed higher levels of ATM (1.4-fold) and Chk2 (1.2-fold) phosphorylation and PARP cleavage (3.7-fold) in LNCaP cells treated with 1 nM R1881 and 500 μM H_2O_2 than in those treated only with 500 μM H_2O_2 (Fig. 3). This androgen-induced PARP cleavage was suppressed by the addition of 10 μM flutamide, which is an inhibitor of the androgen receptor. The expression of androgen receptor was increased by 1 nM R1881, but concomitant treatment with flutamide did not suppress the effects of 1 nM R1881 on androgen receptor levels. We also assessed whether dihydrotestosterone induced ATM phosphorylation (Fig. 4). Levels of ATM phosphorylation and PARP cleavage were 1.9-fold and 3.0-fold higher,

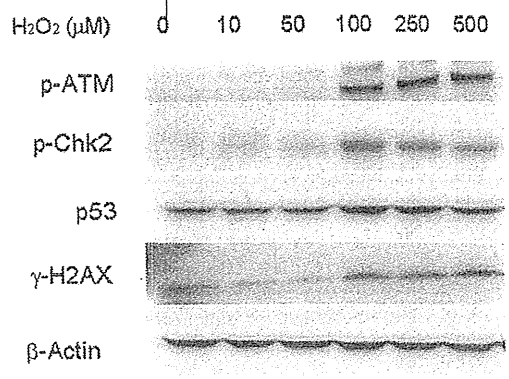

Fig. 2. H_2O_2 induced phosphorylation of ATM, Chk2, p53, and H2AX in LNCaP cells. Protein expression was detected by immunoblotting after 24-h H_2O_2 treatment. Immunoblots were probed with mouse anti-human β-actin antibody as an internal control.

respectively, in LNCaP cells treated with 1 μM dihydrotestosterone and 500 μM H_2O_2 than in those treated only with 500 μM H_2O_2. Ku55933, the ATM inhibitor, reduced the dihydrotestosterone-induced increase in PARP cleavage in LNCaP cells. We also observed the phosphrylation of ATM and induction of PARP cleavage induced by H_2O_2 treatment in 22Rv1 cells (Fig. 5A). Flutamide and Ku55933 reduced the 10 nM dihydrotestosterone-induced increase in PARP cleavage in 22Rv1 cells (Fig. 5B) and LNCaP cells (data not shown). Although synthetic androgen R1881 is not metabolized in the culture medium, 1 nM R1881 is estimated 0.28 ng/ml of testosterone. Ten nanometer dihydrotestosterone is estimated 2.9 ng/ml that is a physiological level of androgen in the prostate tissues.

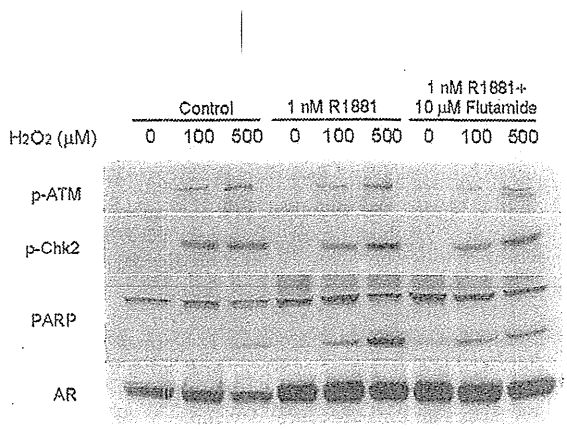

Fig. 3. Synthetic androgen 1 nM R1881 induced the activation of the DNA damage response in H_2O_2-treated cells. p-ATM, phosphorylated-ATM; p-Chk2, phosphorylated-Chk2; PARP, poly (ADP-ribose) polymerase; AR, androgen receptor.

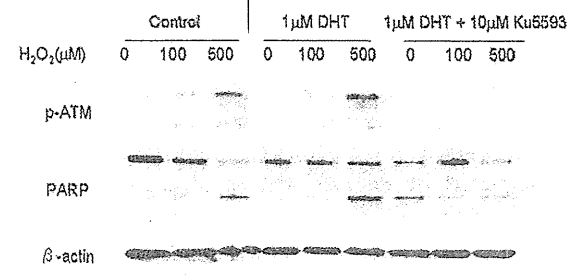

Fig. 4. Dihydrotestosterone induced PARP cleavage with the activation of ATM in LNCaP cells. Immunoblots were probed with mouse anti-human β-actin antibody as an internal control. DHT, dihydrotestosterone; p-ATM, phosphorylated-ATM; PARP, poly (ADP-ribose) polymerase.

DISCUSSION

Prostate cancer is more common in older men, and, as human life expectancy increases, the incidence of prostate cancer is expected to increase. Therefore, the management and prevention of malignant prostate cancer is an increasingly important clinical issue. The Prostate Cancer Prevention Trial (PCPT) [11] and Reduction by Dutasteride of Prostate Cancer Events

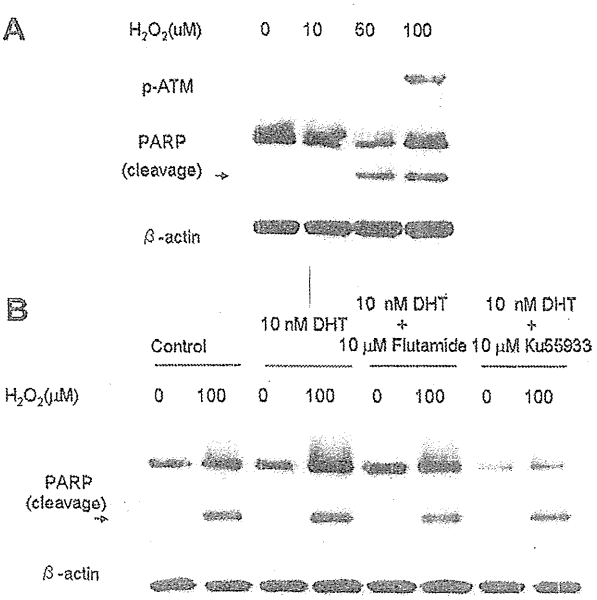

Fig. 5. **A**: H_2O_2 induced PARP cleavage with the activation of ATM in 22Rv-1 cells. **B**: 10 nM dihydrotestosterone induced PARP cleavage with the activation of ATM in 22Rv-1 cells. Immunoblots were probed with mouse anti-human β-actin antibody as an internal control. DHT, dihydrotestosterone; p-ATM, phosphorylated-ATM; PARP, poly (ADP-ribose) polymerase.

(REDUCE) trial [12] have shown that 5-α reductase inhibitors are the only agent class proven to be effective in preventing prostate cancer. However, while finasteride reduced the 7-year period prevalence of prostate cancer, it paradoxically also caused an apparent increase in the proportion of high-grade cases (Gleason score, 7–10) [11]. Till date, about 20 prospective studies have investigated the relationship between endogenous circulating levels of androgens and risk of prostate cancer. Most of these studies have not shown a consistent association between high circulating levels of androgens and increased risk of prostate cancer [1]. Moreover, low testosterone levels have been shown to be associated with an advanced tumor stage at presentation, positive surgical margins, high Gleason scores, and worse overall survival [2,13]. There is increasing evidence both from epidemiological studies and animal models that specific endocrine-disrupting compounds may influence the development or progression of prostate cancer. However, the exact mechanisms underlying androgen-mediated inhibition of malignant transformation in prostate cells have not been fully elucidated.

Prostate carcinogenesis and prostate cancer progression represent a continuum of genetic and phenotypic alterations. Oxidative stress is associated with DNA damage, and various key gene targets, including components of the DNA damage response pathway, are subject to genomic alteration in prostate cancer. ATM plays important roles in the maintenance of the cell homeostasis in response to oxidative stress, and its downstream target, γH2AX, repairs DNA damage, including the damage induced by oxidative stress [8]. Immunohistochemical studies show that ATM and Chk2 activation at early stages of prostate tumorigenesis suppresses tumor progression and that attenuation of ATM activation promotes cancer progression [9]. In addition, the risk of prostate cancer is known to be elevated in carriers of ATM polymorphisms and Chk2 mutations [14,15]. Our findings demonstrated that androgens induced the DNA damage response in prostate cancer cells subjected to oxidative stress. If the loss of expression or mutations of these proteins were occurred, impaired DNA damage response may allow cancer development. Furthermore, testosterone is not able to contribute the preventive effects on carcinogenesis through DNA damage response. Further studies should be directed at confirming of the role of testosterone and defining how the ATM-Chk2-H2AX pathway functions in the cellular response to oxidative stress. The modulation of oxidative stress and DNA damage response pathways may be an effective strategy to prevent or delay the onset of prostate cancer.

REFERENCES

1. Wiren S, Stattin P. Androgens and prostate cancer risk. Best Pract Res Clin Endocrinol Metab 2008;22(4):601–613.
2. Imamoto T, Suzuki H, Yano M, Kawamura K, Kamiya N, Araki K, Komiya A, Nihei N, Naya Y, Ichikawa T. The role of testosterone in the pathogenesis of prostate cancer. Int J Urol 2008; 15(6):472–480.
3. Morris MJ, Huang D, Kelly WK, Slovin SF, Stephenson RD, Eicher C, Delacruz A, Curley T, Schwartz LH, Scher HI. Phase 1 trial of high-dose exogenous testosterone in patients with castration-resistant metastatic prostate cancer. Eur Urol 2009; 56(2):237–244.
4. Szmulewitz R, Mohile S, Posadas E, Kunnavakkam R, Karrison T, Manchen E, Stadler WM. A randomized phase 1 study of testosterone replacement for patients with low-risk castration-resistant prostate cancer. Eur Urol 2009;56(1):97–103.
5. Malins DC, Johnson PM, Wheeler TM, Barker EA, Polissar NL, Vinson MA. Age-related radical-induced DNA damage is linked to prostate cancer. Cancer Res 2001;61(16):6025–6028.
6. Malins DC, Johnson PM, Barker EA, Polissar NL, Wheeler TM, Anderson KM. Cancer-related changes in prostate DNA as men age and early identification of metastasis in primary prostate tumors. Proc Natl Acad Sci USA 2003;100(9):5401–5406.
7. Bartek J, Bartkova J, Lukas J. DNA damage signalling guards against activated oncogenes and tumour progression. Oncogene 2007;26(56):7773–7779.
8. Jackson SP, Bartek J. The DNA-damage response in human biology and disease. Nature 2009;461(7267):1071–1078.
9. Fan C, Quan R, Feng X, Gillis A, He L, Matsumoto ED, Salama S, Cutz JC, Kapoor A, Tang D. ATM activation is accompanied with earlier stages of prostate tumorigenesis. Biochim Biophys Acta 2006;1763(10):1090–1097.
10. Valavanidis A, Vlachogianni T, Fiotakis C. 8-hydroxy-2' -deoxyguanosine (8-OHdG): A critical biomarker of oxidative stress and carcinogenesis. J Environ Sci Health C Environ Carcinog Ecotoxicol Rev 2009;27(2):120–139.
11. Thompson IM, Goodman PJ, Tangen CM, Lucia MS, Miller GJ, Ford LG, Lieber MM, Cespedes RD, Atkins JN, Lippman SM, Carlin SM, Ryan A, Szczepanek CM, Crowley JJ, Coltman CA Jr. The influence of finasteride on the development of prostate cancer. N Engl J Med 2003;349(3):215–224.
12. Andriole G, Bostwick D, Brawley O, Gomella L, Marberger M, Tindall D, Breed S, Somerville M, Rittmaster R. Chemoprevention of prostate cancer in men at high risk: Rationale and design of the reduction by dutasteride of prostate cancer events (REDUCE) trial. J Urol 2004;172(4 Pt 1):1314–1317.
13. Ide H, Yasuda M, Nishio K, Saito K, Isotani S, Kamiyama Y, Muto S, Horie S. Development of a nomogram for predicting high-grade prostate cancer on biopsy: The significance of serum testosterone levels. Anticancer Res 2008;28(4C):2487–2492.
14. Angele S, Falconer A, Edwards SM, Dork T, Bremer M, Moullan N, Chapot B, Muir K, Houlston R, Norman AR, Bullock S, Hope Q, Meitz J, Dearnaley D, Dowe A, Southgate C, Ardern-Jones A, Easton DF, Eeles RA, Hall J. ATM polymorphisms as risk factors for prostate cancer development. Br J Cancer 2004; 91(4):783–787.
15. Wu X, Dong X, Liu W, Chen J. Characterization of CHEK2 mutations in prostate cancer. Hum Mutat 2006;27(8):742–747.

OPEN ACCESS Freely available online

PLoS one

Cure of ADPKD by Selection for Spontaneous Genetic Repair Events in *Pkd1*-Mutated iPS Cells

Li-Tao Cheng[1,2], Shogo Nagata[1,3], Kunio Hirano[1], Shinpei Yamaguchi[1,3], Shigeo Horie[4], Justin Ainscough[5], Takashi Tada[1,3]*

1 Stem Cell Engineering, Institute for Frontier Medical Sciences, Kyoto University, Kyoto Japan, 2 Department of Nephrology, Peking University Third Hospital, Beijing, China, 3 JST CREST, Kawaguchi, Saitama, Japan, 4 Department of Urology, Teikyo University, Tokyo, Japan, 5 Cardiovascular and Neuronal Remodelling, LIGHT, Leeds University, Leeds, United Kingdom

Abstract

Induced pluripotent stem cells (iPSCs) generated by epigenetic reprogramming of personal somatic cells have limited therapeutic capacity for patients suffering from genetic disorders. Here we demonstrate restoration of a genomic mutation heterozygous for *Pkd1* (polycystic kidney disease 1) deletion (Pkd1(+/−) to Pkd1(+/R+)) by spontaneous mitotic recombination. Notably, recombination between homologous chromosomes occurred at a frequency of 1~2 per 10,000 iPSCs. Southern blot hybridization and genomic PCR analyses demonstrated that the genotype of the mutation-restored iPSCs was indistinguishable from that of the wild-type cells. Importantly, the frequency of cyst generation in kidneys of adult chimeric mice containing Pkd1(+/R+) iPSCs was significantly lower than that of adult chimeric mice with parental Pkd1(+/−) iPSCs, and indistinguishable from that of wild-type mice. This repair step could be directly incorporated into iPSC development programmes prior to cell transplantation, offering an invaluable step forward for patients carrying a wide range of genetic disorders.

Citation: Cheng L-T, Nagata S, Hirano K, Yamaguchi S, Horie S, et al. (2012) Cure of ADPKD by Selection for Spontaneous Genetic Repair Events in *Pkd1*-Mutated iPS Cells. PLoS ONE 7(2): e32018. doi:10.1371/journal.pone.0032018

Editor: Martin Pera, University of Southern California, United States of America

Received October 11, 2011; **Accepted** January 17, 2012; **Published** February 9, 2012

Funding: This work was funded by grants from the Japan Society for the Promotion of Science, the Ministry of Education, Culture, Sports, Science and Technology and the Core Research for Evolutional Science and Technology (Japan Science and Technology Agency) to TT, and the Takeda Science foundation to LC. The funders had no role in study design, data collection and analysis, decision to publish, or preparation of the manuscript.

Competing Interests: The authors have declared that no competing interests exist.

* E-mail: ttada@frontier.kyoto-u.ac.jp

Introduction

Epigenetic reprogramming of personal somatic cells into iPSCs by forced expression of defined transcription factors confers pluripotency [1–3], but does not restore mutations that cause genetic disorders. For therapeutic treatment of genetic disorders, techniques using plasmid, zinc finger nucleases and helper-dependent adenoviral vector-mediated homologous recombination have been developed to induce genetic editing in disease-specific iPSCs and embryonic stem cells (ESCs) [4–9]. The requirement for target gene-specific vectors coupled with inherent low efficiency has restricted translation of the theoretical possibilities to practical application of these techniques in iPSCs for clinical therapy. Furthermore, Genetic modification in iPSCs gives an obstacle to safety in clinical applications. Mitotic recombination, which functions in DNA repair [10], occurs at a low frequency ($<10^{-6}$) in somatic cells [11]. However, in experiments to drive targeted chromosome elimination from pluripotent ES-somatic hybrid cells [12], evidence suggested the frequency of genetic repair events through spontaneous mitotic recombination in pluripotent stem cells is higher than that in somatic cells [11]. Furthermore, chromosome-specific loss of heterozygosity was created in a KO allele by high-dose G418 selection to the *Neo* gene in mouse embryonic stem cells [13]. Thus, we investigated whether it was possible to identify and propagate isogenic clones of iPSCs, which retain the property of infinite cell proliferation, in which spontaneously genetic correction had occurred at disease-related mutation alleles through mitotic recombination (Figure 1).

Here, to demonstrate proof of principle for this theoretical approach, we have investigated a prevalent inherited disorder, autosomal dominant polycystic kidney disease (ADPKD). ADPKD, which is caused by genetic mutation of the *PKD1* and *PKD2* gene in 85% and 15% of cases, respectively [14], is clinically diagnosed by intrarenal cystogenesis caused by complex mechanisms. Deregulation of *PKD1* or *PKD2*-coding polycystin protein level results in initiation of cyst formation, followed by several signaling pathways that mediate cyst growth and expansion [15].

Results and Discussion

iPSC lines were generated from mouse embryonic fibroblasts (MEFs) derived from E12.5 *Pkd1* knockout (KO)-heterozygous embryos [16], through retroviral transduction of *Oct4*, *Sox2*, and *Klf4* (OSK) (Figure 1). The embryos were obtained by mating C57BL/6 wild-type (+/+) mice with C57BL/6 *Pkd1*(+/−) mice. Male *Pkd1*(+/−) MEFs were selected by genomic PCR analysis of the Y-chromosome-specific *Zfy* gene prior to OSK viral transfection (Figure S1). Male iPSC lines, which were re-cloned following GFP transfection, retained normal colony morphology and stable expression of GFP marker (Figure 2a). Normal karyotype, $2n = 40XY$, was observed in 93 out of 104 (89.4%) cells examined (Figure S2). Pluripotency of Pkd1(+/−) iPSCs was validated by expression of pluripotent marker proteins, Oct4, Sox2, and Nanog

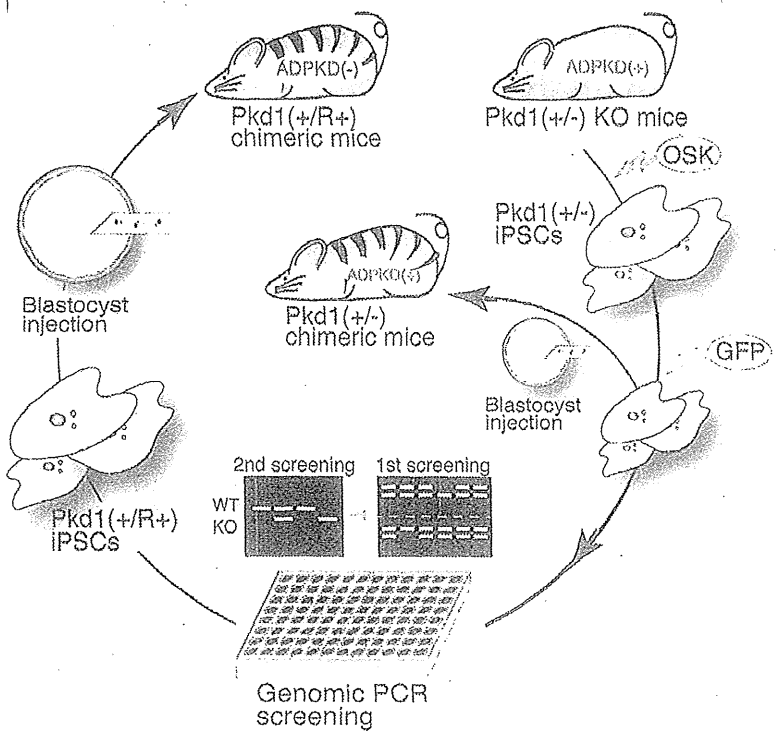

Figure 1. Scheme of in vitro screening and in vivo assay of mutation-restored Pkd1(+/R+) iPSCs. The knockout (KO) allele of *Pkd1* is spontaneously replaced with the wild-type allele through mitotic recombination occurring in rounds of cell division of Pkd1(+/−) iPSCs. Phenotype of ADPKD (autosomal dominant polycystic kidney disease) caused by the mutation of *Pkd1* is detected in kidneys from adult chimeric mice with Pkd1(+/−), but not Pkd1(+/R+), iPSCs.
doi:10.137˙/journal.pone.0032018.g001

by immunohistochemistry (Figure 2b), and transcription of pluripotent marker genes, *Oct4*, *Sox2*, *Klf4*, *Nanog*, *Rex1*, *Gdf3*, *Sall4*, *Dnmt3b*, *Klf2*, and *Dax1* by RT-PCR (Figure 2c). Colonies amplified from single Pkd1(+/−) iPSCs by plating sparsely into 10 cm dishes were picked, expanded and screened by genomic PCR using a *Pkd1*-specific primer set (Figure 1). Candidate clones were secondary screened by genomic PCR with an additional primer set specific to the KO allele-specific *Neo* gene (Figure 2d). In total, more than 10,000 independent colonies were screened by genomic PCR. Interestingly, two Pkd1(+/R+) clones lacking the KO allele (Figure 2d), and one Pkd1(R−/−) clone lacking the wild-type allele were detected. The frequency of spontaneous mitotic recombination-mediated mutation repair event between homologous chromosomes was estimated at 1.94×10^{-4} for Pkd1(+/R+) clone and 0.97×10^{-4} for Pkd1(R−/−) clone (Table 1). The spontaneous repair events between homologous chromosomes occurred at the frequency, which could be applicable to clinical applications.

To address the mechanism of allelic exchange at the *Pkd1* locus, DNA extracted from Pkd1(+/R+) iPSC lines was analyzed by Southern blot hybridization with probe 1, 2, and 3 (Figure 2e). Fragments for the KO allele, 7.8 kb with probe 1 and 7.0 kb with probe 3, were detected in Pkd1(+/−) iPSCs but not wild-type or Pkd1(+/R+) iPSCs, confirming loss of the *Neo* containing region. The intensity of the 15.1 kb band for the wild-type allele, detected by all three probes, was similar between wild-type and Pkd1(+/R+) iPSCs, and reduced by approximately 50% in Pkd1(+/−) iPSCs, when normalized against an internal loading control *Stella*, demonstrating replacement of the KO allele with the wild-type allele through mitotic recombination. To exclude the possibility of wild-type cell contamination as a source of apparent Pkd1(+/R+) iPSCs, Southern blot hybridization was performed with a probe specific to *Klf4* integrated as a multi-copy transgene in the iPSC genome but not the wild-type genome (Figure 2f). Detection of the same pattern of multiple bands in Pkd1(+/−) and Pkd1(+/R+) iPSCs demonstrates that Pkd1(+/R+) iPSCs originated from Pkd1(+/−) iPSCs.

To investigate the influence of mitotic recombination on *Pkd1* expression, mRNA levels were analyzed by RT-PCR (Figure S3). Expression in Pkd1(+/−) iPSCs was approximately half that in WT or Pkd1(+/R+) iPSCs. Thus, expression of *Pkd1* was restored to the normal level in Pkd1(+/R+) iPSCs. Next, to examine physiological effects of the restoration of the KO to wild-type allele, chimeric mice were generated with Pkd1(+/−) and Pkd1(+/R+) iPSCs, both of which exhibit ubiquitous GFP expression (Figure 3a). Chimeras were analyzed at more than 6 months old following established criteria for cystogenesis as reported previously, i.e. cyst diameter >200 μm [17]. Kidneys collected in triplicate from mice generated with wild-type, Pkd1(+/−), and Pkd1(+/R+) chimeric genotypes were sacrificed for histological analyses. Extent of chimerism (22∼48%) was comparable between Pkd1(+/−) and Pkd1(+/R+) kidneys we examined (Figure 3b). Cyst formation was frequently detected in the cortical region of the Pkd1(+/−) chimeric kidneys but not the Pkd1(+/R+) and wild-type kidneys (Figure S4). GFP-positive cells comprising part of the cyst wall were observed in Pkd1(+/−) chimeric kidneys (Figure 3c), indicating that unbalanced expression level of polycystin protein in Pkd1(+/−) kidney cells might induce to initiate the cystogensis.

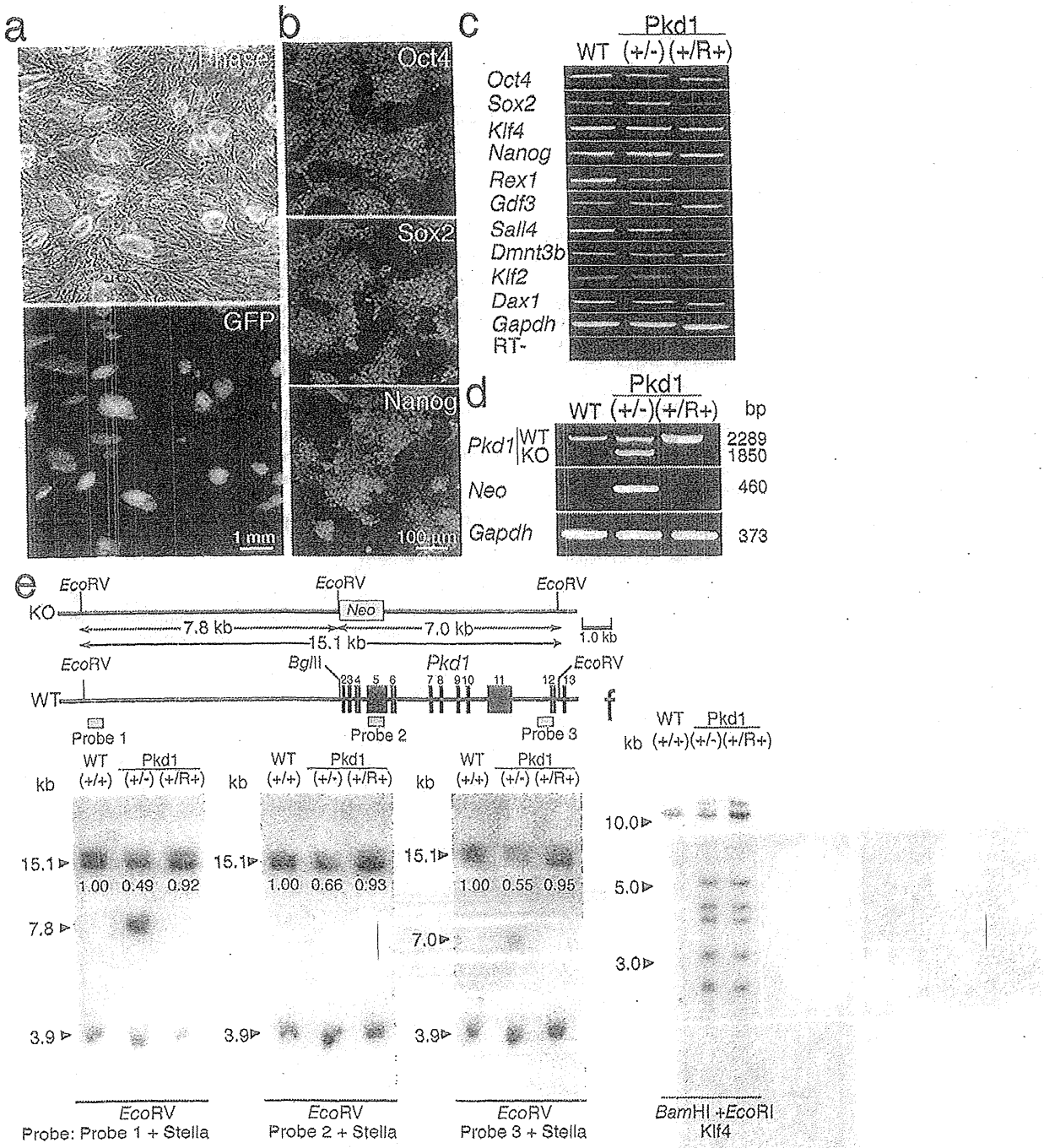

Figure 2. Screening of mutation-restored (Pkd1(+/R+)) iPSCs from iPSCs heterozygous for *Pkd1* knockout (KO) (Pkd1(+/−)). **a,** Normal colony morphology of Pkd1(+/−) iPSCs expressing fluorescence marker protein, GFP. **b,** Expression of pluripotent marker proteins, Oct4, Sox2, and Nanog in Pkd1(+/R+) iPSCs by immunohistochemical analyses. **c,** Transcription of pluripotent marker genes in Pkd1(+/−) and Pkd1(+/R+) iPSCs by RT-PCR analyses. **d,** Secondary screening of Pkd1(+/R+) iPSCs by genomic PCR analyses. **e,** Verification of replacement of the KO allele by the wild-type (WT) allele through spontaneous mitotic recombination in Pkd1(+/R+) iPSCs by Southern blot hybridization analyses. Relative intensity is noted under the 15.1 kb band. **f,** Determination of the origin of Pkd1(+/R+) iPSCs by Southern blot hybridization.
doi:10.1371/journal.pone.0032018.g002

Notably, the frequency of cyst formation was more than ten times higher in Pkd1(+/−), than Pkd1(+/R+) chimeric kidneys (Figure 3d). The number of cysts detected in Pkd1(+/R+) chimeric kidneys was comparable to that in wild-type kidneys. These data clearly demonstrate that the mutation in Pkd1(+/−) iPSCs involved in ADPKD was genetically and functionally restored in Pkd1(+/R+) iPSCs through spontaneous mitotic recombination. It is evident that selection of genetic mutation-restored iPSCs by

Table 1. Frequency of spontaneous mitotic recombination at *Pkd1* KO allele in iPSCs.

No. of colonies			
Picked up	PCR analyzed (%)	Pkd1(+/R+) (Frequency)	Pkd1(R−/−) (Frequency)
11,232	10,322 (91.9)	2 (1.94×10^{-4})	1 (0.97×10^{-4})

doi:10.1371/journal.pone.0032018.t001

spontaneous mitotic recombination is a realistic way to isolate isogenic and functionally restored iPSCs safely for using clinical applications.

Our results establish a paradigm for enrichment of iPSC clones, by large-scale screening, in which restoration of genetic disorder-inducing mutations has occurred spontaneously through mitotic recombination. The frequency of spontaneous mitotic recombination may not be estimated properly in pluripotent stem cells and embryonic cells in vivo and in vitro, since the event occurring in a tiny number of cells was detected using a G418-resistant selection with the *Neo* gene in many cases. In fact, mouse ESCs homozygous for the *Neo*-tagged chromosomes were selected and expanded from ESCs heterozygous for *Neo*-tagged chromosome by the high dose treatment of G418 at the frequency of approximately 1×10^{-6} [12–13]. The generation frequency of G418-resistant cells may be underestimated to that of homologous mitotic recombination, since some pluripotent stem cells homozygous for *Neo*, expressing insufficient amount of gene product, could stop growing or be killed. FACS analysis of mouse ESCs heterozygous for the *GFP* reporter gene without drug selection detected GFP-negative cells at the frequency of about 1×10^{-3} (data not shown), which were generated by homologous mitotic recombination or deletion of the *GFP* gene. The circumstance evidence supports that mitotic homologous recombination at an allele occurs at the frequency of about $1\times10^{-4}\sim10^{-5}$, similar to our findings using iPSCs. If so, the genetic information may diverge between somatic cells thorough cell divisions rather than we predicted.

An automatic genome-sorting system could make screening of mitotic recombination-mediated genetic correction feasible. Importantly, this approach dispenses with requirement for gene therapy. As with mutation-dominant diseases such as ADPKD and LEOPARD syndrome [18], the approach is similarly applicable to genetic mutations in recessive diseases [19]. Once generated, the disease-repaired iPSCs may be useful for regenerative medicine as well as other applications. Thus, the mitotic recombination-mediated genetic correction approach will open a new path to clinical application for human iPSCs that is relevant to patient groups, for which the iPSC technological revolution was believed to hold little relevance in the clinical setting.

Materials and Methods

Ethics statement

Experiments with mice were performed according to the institutional guideline of Kyoto University, Japan. Our animal experiments (W-3-6) are reviewed and permitted by the animal research committee of Kyoto University, JAPAN.

Cell culture

Pkd1(+/−) iPSC lines were established from male MEFs of E12.5 *Pkd1* knockout mouse embryos [16] by retroviral transduction of mouse OSK [20]. iPSC lines were maintained in mES medium (DMEM/F12 supplemented with 15% FBS, L-glutamine, penicillin-streptomycin, sodium bicarbonate, sodium pyruvate, 2-

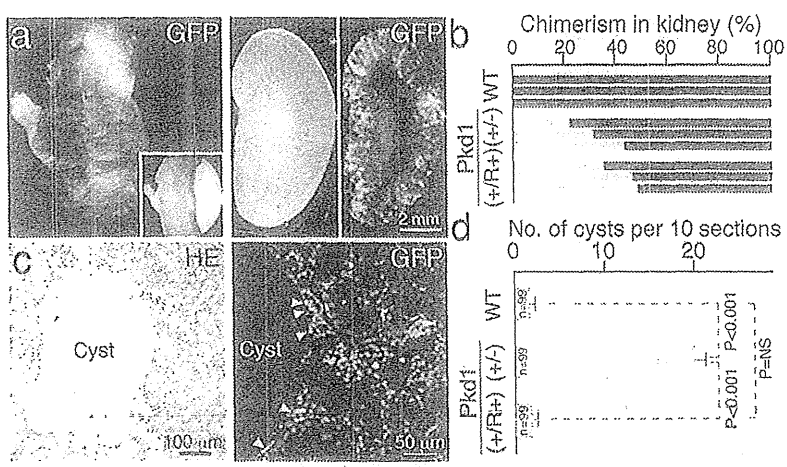

Figure 3. Restoration of ADPKD phenotype in adult chimeric mice with Pkd1(+/R+) iPSCs. a, Newborn chimeric mouse (green) generated by micro injection of Pkd1(+/−) iPSCs into host blastocyst (left panel). Contribution of Pkd1(+/R+) iPSCs into a chimeric kidney is visualized by GFP expression (right panel). **b,** Contribution of iPSCs into chimeric kidneys. Degree of iPSC contribution to each kidney collected from different chimeric mouse with Pkd1(+/−), or Pkd1(+/R+) iPSCs is indicated by a green bar. **c,** A hematoxylin-eosin (HE) section of Pkd1(+/−) chimeric kidney. A cyst was recognized as diameter greater than 200 μm (left panel). Pkd1(+/−)iPSC-derived cells (green) are located on the cyst wall (white arrow heads in right panel). Nuclei are stained as blue by DAPI. **d,** Frequency of cyst generation in kidneys from Pkd1(+/−), or Pkd1(+/R+) iPSC chimeric mice. The number of cysts was counted on HE sections of kidneys, in which degree of chimerism was estimated by GFP analysis in **b** (33 sections from each kidney). Error bars, s.e.m.

doi:10.1371/journal.pone.0032018.g003

mercaptoethanol and 1000 U/ml of LIF (Chemicon, Temecula, CA, USA)). For isolating colonies originated from single cells, about 600 cells were plated into each 10 cm culture dish. The *EGFP* gene was introduced into Pkd1(+/−) iPSCs by lentiviral transduction.

Chromosome

Cells were treated with 0.075 M KCl for 8 min at room temperature and then fixed in 3:1 methanol:acetic acid. Slides of chromosomes prepared by an air-drying method were stained with Hoechst 33258 (10 ng/ml) for G-banding analysis.

Genomic and RT-PCR

PCR primers used in this study are listed in Table S1. For Genomic PCR, products were amplified with GoTaq (Promega) by 35 cycles of reactions. For RT-PCR, total RNA of cultured cells was extracted with TRIzol reagent (Invitrogen, USA). cDNA was synthesized from 500 ng of total RNA with Superscript III (Invitrogen, USA) using random hexamers following manufacturers instructions. Band intensity was measured using Image J (NIH).

Southern blot hybridization

Genomic DNAs was digested with restriction enzyme(s), separated by electrophoresis on a 1.0% agarose gel, and transferred on a Hybond N^+ filter by alkali blotting. The membrane was hybridized with probes labeled with ^{32}P using the Megaprime DNA labeling system (Amersham) overnight at 42°C following pre-hybridization treatment. The membrane was washed twice in 2×SSC/0.1% SDS at 65°C for 30 minutes and twice in 0.1×SSC/0.1% SDS at 65°C for 15 minutes. Band intensity was measured using Image J.

Chimera

For producing chimeric embryos, Pkd1(+/−) and Pkd1(+/R+) iPSCs ubiquitously expressing *EGFP*, were microinjected into C57BL/6J×BDF1 blastocysts. 6–18 months old chimeric mice were sacrificed for histological analyses.

Histology

For immunocytochemistry, cultured cells were fixed with 4% PFA (paraformaldehyde)/PBS (phosphate-buffered saline) for 10 minutes at room temperature, washed with PBST (0.1% Triton X-100 in PBS), then pre-treated with blocking solution (3% BSA and 2% skimmed milk (DIFCO, USA) in PBST) at 4°C overnight. The cells were then stained with fluorescence-conjugated secondary antibodies (1:500, Invitrogen), following immuno-reaction with primary antibodies; anti-OCT4 (1:50, Santa Cruz Biotechnology, USA), anti-SOX2 (1:500, Abcam, Cambridge, UK), and anti-NANOG (1:200, ReproCELL, Japan). The cells were counterstained with DAPI (4,6-diamidino-2-phenylindole) and mounted with SlowFade light antifade kit (Invitrogen). Kidneys from 6–18 month old mice were fixed with 4% PFA/PBS for 4–6 hours, and embedded in paraffin. Sections at 5 μm in thickness were stained with haematoxylin and eosin.

Supporting Information

Figure S1 Genotyping of mouse embryonic fibroblasts (MEFs) from E12.5 embryos generated by mating of wild-type (WT) and Pkd1(+/−) mice. *Zfy* is PCR product specific to male. M; male, F; female. Male MEFs (no. 2) heterozygous for *Pkd1* knockout (KO) was used for iPSC generation.
(TIF)

Figure S2 Karyotype of Pkd1(+/R+) iPSC. Normal karyotype, $2n = 40$,XY is shown chromosomally.
(TIF)

Figure S3 Transcription of Pkd1 mRNA in Pkd1(+/−) and Pkd1(+/R+) iPSCs. Transcription level of mRNA compared by band intensity is comparable between wild-type (WT) and mutation restored Pkd1(+/R+) iPSCs, while is an approximately half of WT in Pkd1(+/−) iPSCs.
(TIF)

Figure S4 Hematoxylin-eosin sections of kidneys at low magnification. Cysts are frequently found in Pkd1(+/−) chimeric kidneys, but not wild-type (WT) and mutation-restored Pkd1(+/R+) chimeric kidneys.
(TIF)

Acknowledgments

We thank Dr Gen Kondoh and Ms Hitomi Watanabe for generating chimeras. L.T.C. is a postdoctoral fellow supported by the Takeda Science Foundation, JAPAN. K.H is a fellow of JSPS.

Author Contributions

Conceived and designed the experiments: TT. Performed the experiments: LC SN KH SY TT. Analyzed the data: LC SN KH SY TT. Contributed reagents/materials/analysis tools: SH. Wrote the paper: JA TT.

References

1. Takahashi K, Yamanaka S (2006) Induction of pluripotent stem cells from mouse embryonic and adult fibroblast cultures by defined factors. Cell 126: 663–676.
2. Takahashi K, Tanabe K, Ohnuki M, Narita M, Ichisaka T, et al. (2007) Induction of pluripotent stem cells from adult human fibroblasts by defined factors. Cell 131: 861–872.
3. Lowry WE, Richter L, Yachechko R, Pyle AD, Tchieu J, et al. (2008) Generation of human induced pluripotent stem cells from dermal fibroblasts. Proc Natl Acad Sci USA 105: 2883–2888.
4. Rideout WM, 3rd, Hochedlinger K, Kyba M, Daley GQ, Jaenisch R (2002) Correction of a genetic defect by nuclear transplantation and combined cell and gene therapy. Cell 109: 17–27.
5. Hockemeyer D, Soldner F, Beard C, Gao Q, Mitalipova M, et al. (2009) Efficient targeting of expressed and silent genes in human ESCs and iPSCs using zinc-finger nucleases. Nat Biotechnol 27: 851–857.
6. Zhou H, Wu S, Joo JY, Zhu S, Han DW, et al. (2009) Generation of induced pluripotent stem cells using recombinant proteins. Cell Stem Cell 4: 381–384.
7. Hockemeyer D, Wang H, Kiani S, Lai CS, Gao Q, et al. (2011) Genetic engineering of human pluripotent cells using TALE nucleases. Nat Biotechnol 29: 731–734.
8. Liu GH, Suzuki K, Qu J, Sancho-Martinez I, Yi F, et al. (2011) Targeted gene correction of laminopathy-associated LMNA mutations in patient-specific iPSCs. Cell Stem Cell 8: 688–694.
9. Soldner F, Laganière J, Cheng AW, Hockemeyer D, Gao Q, et al. (2011) Generation of isogenic pluripotent stem cells differing exclusively at two early onset Parkinson point mutations. Cell 146: 318–331.
10. Moynahan ME, Jasin M (2010) Mitotic homologous recombination maintains genomic stability and suppresses tumorigenesis. Nat Rev Mol Cell Biol 11: 196–207.
11. Kipps TJ, Herzenberg LA (1986) Homologous chromosome recombination generating immunoglobulin allotype and isotype switch variants. Embo J 5: 263–268.
12. Matsumura H, Tada M, Otsuji T, Yasuchika K, Nakatsuji N, et al. (2007) Targeted chromosome elimination from ES-somatic hybrid cells. Nat Methods 4: 23–25.
13. Lefebvre L, Dionne N, Karaskova J, Squire JA, Nagy A (2001) Selection for transgene homozygosity in embryonic stem cells results in extensive loss of heterozygosity. Nat Genet 27: 257–258.
14. Chapin HC, Caplan MJ (2010) The cell biology of polycystic kidney disease. J Cell Biol 191: 701–710.

15. Happe H, de Heer E, Peters DJ (2011) Polycystic kidney disease: The complexity of planar cell polarity and signaling during tissue regeneration and cyst formation. Biochim Biophys Acta 1812: 1249–1255.
16. Muto S, Aiba A, Saito Y, Nakao K, Nakamura K, et al. (2002) Pioglitazone improves the phenotype and molecular defects of a targeted Pkd1 mutant. Hum Mol Genet 11: 1731–1742.
17. Gardner KD, Jr. (1988) Pathogenesis of human cystic renal disease. Annu Rev Med 39: 185–191.
18. Carvajal-Vergara X, Sevilla A, D'Souza SL, Ang YS, Schaniel C, et al. (2010) Patient-specific induced pluripotent stem-cell-derived models of LEOPARD syndrome. Nature 465: 808–812.
19. Park IH, Arora N, Huo H, Maherali N, Ahfeldt T, et al. (2008) Disease-specific induced pluripotent stem cells. Cell 134: 877–886.
20. Nagata S, Toyoda M, Yamaguchi S, Hirano K, Makino H, et al. (2009) Efficient reprogramming of human and mouse primary extra-embryonic. cells to pluripotent stem cells. Genes Cells 14: 1395–1404.

Revised version

老年症候群の適切な把握のためのもの忘れセンター予診票の作成に関する検討

ー予診票の妥当性と信頼性および回答者による回答率の差異についての検証ー

所属：杏林大学医学部高齢医学

著者：永井久美子、小柴ひとみ、小林義雄、山田如子、須藤紀子、長谷川浩、松井敏史、神崎恒一

Running title：老年症候群把握のためのもの忘れセンター予診票の作成と検証

連絡先：永井久美子

〒181-8611

東京都三鷹市新川 6-20-2　杏林大学医学部高齢医学教室

Tel　：0422-47-5511

Fax　：0422-44-1917

E-mail　　:kobakumi@ks.kyorin-u.ac.jp

要旨

【目的】

加齢に伴い出現する老年症候群を適切に把握することは、高齢者の診療にとって重要である。今回我々はより具体的かつ正確に評価することを目的として予診票の改訂を行い、妥当性および信頼性を検討した。

【方法】

対象は杏林大学病院もの忘れセンター初診患者。2011 年 10 月～2012 年 7 月の初診患者 459 人には従前の質問形式による旧予診票を、2012 年 8 月～12 月の初診患者 277 人には新予診票を診察前に渡し、患者本人もしくは家族その他の同伴者が記入の上、老年症候群の有無を調査した。新予診票の質問項目は各種ガイドラインの診断基準を参考にし、具体的かつ専門用語の使用を控えた「はい／いいえ」で答える 17 項目とした。対象者にはその後高齢者総合機能評価(CGA)を試行し、新予診票の構成概念妥当性および因子妥当性を検討した。また、旧／新予診票間での各質問項目の陽性回答率の比較のほか、新予診票を活用する際に、回答者が本人の場合と同伴者の場合とで陽性回答率に違いが見られるかどうかについても併せて検討した。

【結果】

対象者における予診票の回収率は 100%であり、旧／新の予診票回答者の年齢・男女比・MMSE 得点など基本属性に差は無かった。新予診票と CGA 各項目との相関を検討したところ、新予診票の 17 項目全てが CGA 各項目のいずれかと少なくとも 1 つの有意な相関を有した。また因子分析の結果 17 項目は 8 つの因子に分類され、いずれも CGA 各項目と有意な相関が認

められた。信頼性に関しては、Cronbach のα係数が 0.729、Guttmann の折半法では係数 0.619 であった。

新／旧予診票ともに、患者が高齢で MMSE 低値なほど同伴者が回答していた。新予診票において本人の訴えが最も多い項目は「不眠」であり、これは同伴者が記入した場合でも同様の陽性率であった。一方、「つまずき」「転倒」「歩行障害」「妄想」では本人よりも同伴者が「あり」と多く回答した。「食欲低下」「尿失禁」は旧予診票では同伴者回答での陽性率が高かったが、新予診票では回答者による差が無くなった。新／旧予診票間の比較では、新予診票での陽性回答率は不眠については上昇し、頻尿では低下した。転倒に関しては、本人の陽性回答率は新／旧予診票で変化がなかったが、同伴者の回答では新予診票で陽性回答率が上昇した。

【結論】

新予診票は物忘れ外来の老年症候群検出のスクリーニングとして十分使用に耐えうる妥当性・信頼性を有すると考えられた。また老年症候群の把握に対しては、単に各症候の有無を質問するよりも、具体的な数字や服薬の有無、その結果困難が生じているかなどを考慮して質問する必要があると同時に、高齢者の身体状況の把握には同伴者の視点が重要であることが示された。

Key words: 老年症候群・予診票・高齢者総合機能評価・妥当性・信頼性

緒言

高齢者の診療において、加齢に伴い出現する老年症候群を適切に評価することは、主病の診断や治療方針決定の上で重要である。また、日常生活上の困難、すなわちADLやQOLの阻害要因把握のためにも重要な課題である。予診の役割も患者の主訴や背景因子を聴取するだけの場ではなく、高齢者診療においては、キーパーソンから患者の病態につながる重要な情報を得られる場であり、高齢者総合機能評価(Comprehensive Geriatric Assessment: CGA)もこの段階から始まっているといっても過言ではない(1, 2)。

老年症候群は「高齢者に多い、あるいは特有な症状所見の総称」であり(3)、大内らにより「加齢変化がなく広い年代で出現する症候」「前期高齢者で増加する症候」「後期高齢者で増加する症候」の3群に分類されること、そのなかでも「後期高齢者で増加する症候」は在宅維持阻害要因となることが報告されている(4)。この報告をもとに筆者らの施設では老年症候群把握のための外来予診票を作成した。質問項目は外来受診高齢者に有用と思われる項目、すなわち「加齢変化がなく広い年代で出現する症候」の中から「めまい」「不眠」「転倒」を、「前期高齢者で増加する症候」から「しびれ」「便秘」「食欲低下」を、「後期高齢者で増加する症候」から「尿失禁」「頻尿」「せん妄」の項目を採用した(5)。2003年に作成して以来もの忘れセンター初診時に使用してきたが、この旧予診票を使用していく中でいくつかの問題点が浮かびあがってきた。

一つは医療側の要請である。[TM1]もの忘れセンターでの診

療が経過するにつれ、神経所見や精神徴候を伴う認知症患者が増えたことや、認知症患者の予後に影響するADLや虚弱の程度を予診段階で把握する必要性が高まってきた。多様な認知症患者が診断・治療を求めて来院するようになり、例えばレビー小体型認知症では認知障害の程度は軽くとも幻視、安静時振戦、無動といった徴候が病初期に出現するし(6)、脳血管性認知症では嚥下障害が転倒とならび重要なADLやQOLの低下因子となることから(7)、患者および家族が日常生活において捉えられる徴候を予診段階で拾い上げる必要性が高まったのである。

もう一つは記入時の問題である。旧予診票の質問は医学的症候を「あり／なし」の形で直接問うもので患者にとって具体的な言葉に翻訳されていなかった。そのため患者や家族が回答する際に判断に窮したのか、無回答の項目が多く見られた。また個々の症候の程度や質に関した質問項目がないために、症候そのものの「あり／なし」が回答者の主観に帰し、後の集計の際のデータの信頼性や客観性に瑕疵が生じる恐れがあった。これは個々の症候に関する質問の評価基準が明確でないためであり、結果として日常生活を老年医学的な観点から把握する上でも、集計したデータの客観性や信頼性を担保する上でも、初診時の老年症候群の存在を適切に評価できていないと考えられた。

そこで今回我々の施設では、旧予診票の「あり／なし」の選択という簡便さを残しつつ質問文の内容とレイアウトを変更した新たな予診票を作成し、この新予診票の妥当性および信頼性を検討した。すなわち、もの忘れセンターにおいて予診に続いて行っているCGAを補完しうるか否かの検討を行っ